Supporting Information for

Tubular TiC Fibre Nanostructures as Supercapacitor Electrode Material with Stable Cycling Life and Wide-Temperature Performance

Xinhui Xia,[a,b] Yongqi Zhang,[a] Dongliang Chao,[a] Qinqin Xiong,[b] Zhanxi Fan,[c] Jiangping Tu,[b] Xili Tong,[d] Hua Zhang,[c] and Hong Jin Fan[a,*]

[a] *School of Physical and Mathematical Sciences, Nanyang Technological University, Singapore 637371, Singapore,*

[b] *State Key Laboratory of Silicon Materials, Key Laboratory of Advanced Materials and Applications for Batteries of Zhejiang Province, and Department of Materials Science and Engineering, Zhejiang University, Hangzhou 310027, China*

[c] *School of Materials Science & Engineering, Nanyang Technological University, Singapore 639798, Singapore*

[d] *State Key Laboratory of Coal Conversion, Institute of Coal Chemistry, Chinese Academy of Science, Taiyuan 030001, P. R. China*

Xinhui Xia and Yongqi Zhang contributed equally to this work.

* Address correspondence to fanhj@ntu.edu.sg (H.J. F)

HFC: (TiC) hollow fibre cloth

CFC: carbon fibre cloth

CFC+CNF: carbon fibre cloth branched with carbon nanofibres

HFNT: (TiC) hollow fibre-nanotube

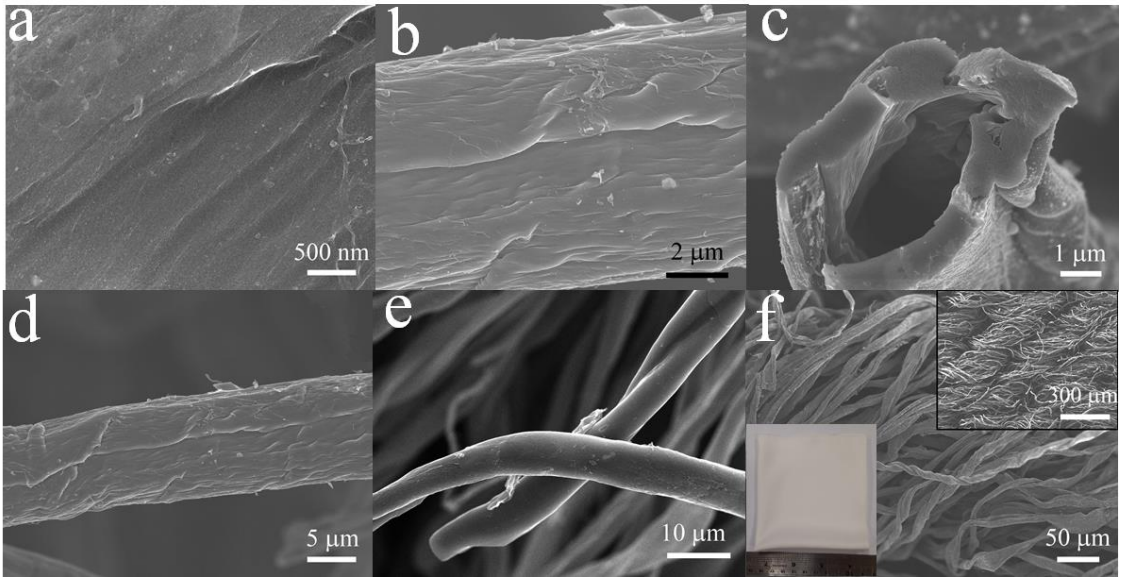

Figure S1 (a-f) SEM images of cotton fibres of commercial cotton T-shirt (Insets: low-magnification SEM image and photo of cotton T-shirt)

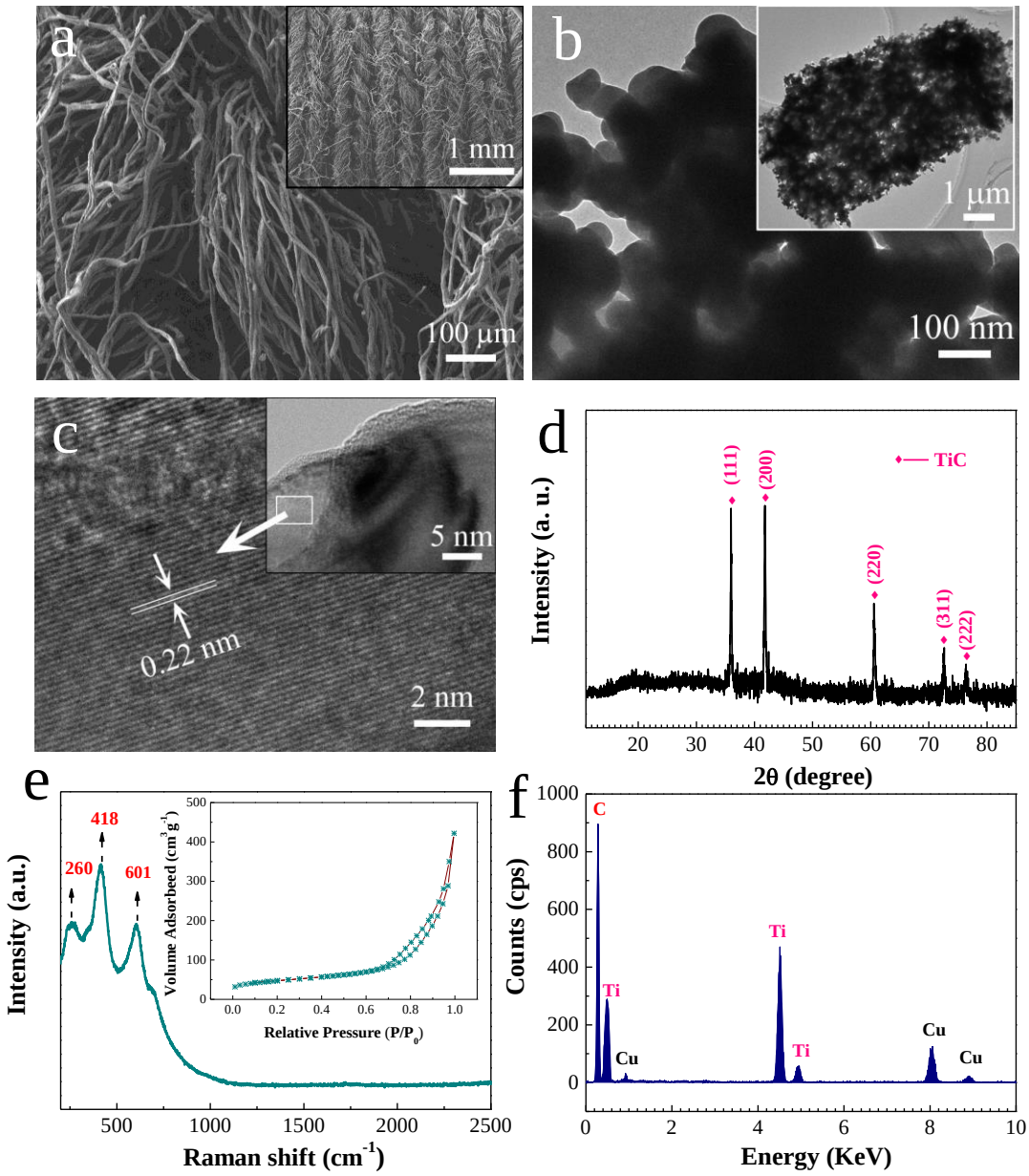

Figure S2 Structural and microstructure characterization of TiC hollow fibres: (a) SEM image of TiC hollow fibre cloth; (b) TEM image (c) and HRTEM of part of one hollow fiber. (d) XRD pattern; (e) Raman spectrum (BET measurement-isothermal curve in inset); (f) EDS spectrum.

XRD pattern (Figure S2d) of the as-prepared TiC HFC electrodes shows five strong diffraction peaks at 35.9, 41.7, 60.5, 72.4, and 76.1°, consistent with JCPDS 65-0242. No other impurity peaks are detected. The phase purity of the as-synthesized samples is also verified by Raman spectrum (Figure S2e). The three typical Raman peaks (260, 418, 601 cm^{-1}) are characteristic of TiC.[1-3] EDS spectrum of the TiC fibres in Figure S2a further confirms the component of Ti and C (Cu signal is from the TEM copper grid).

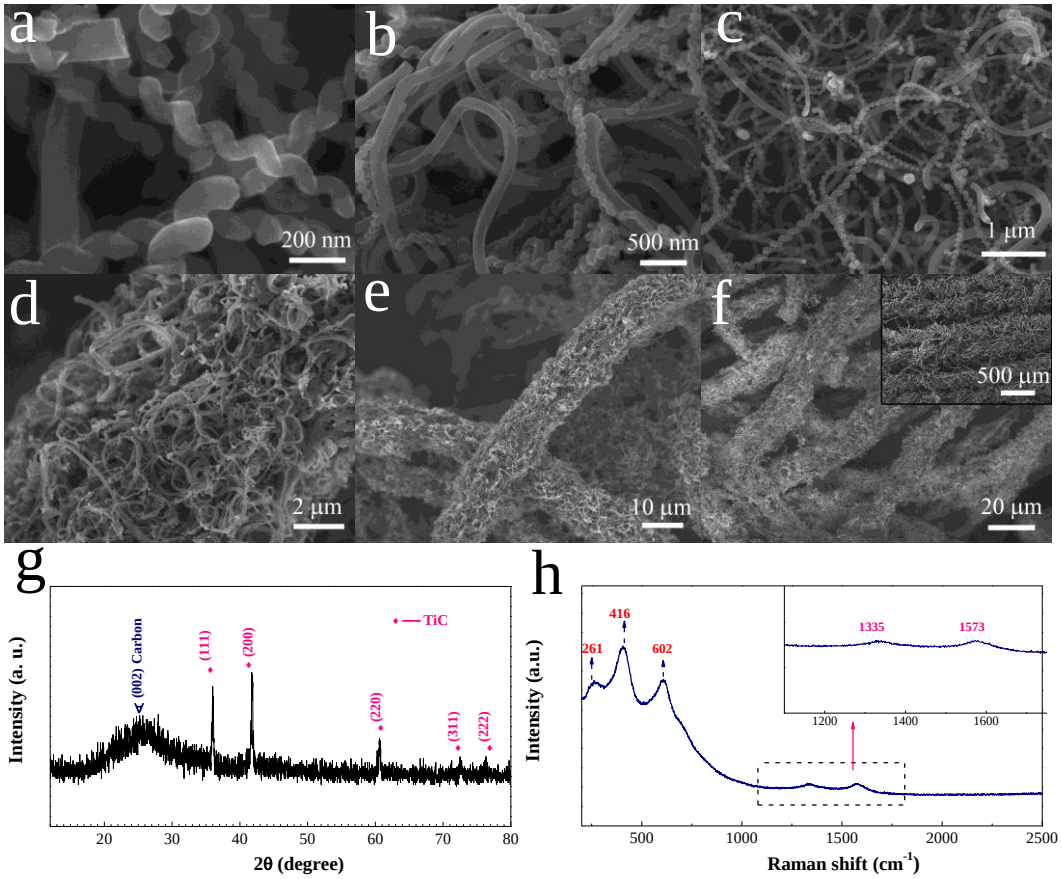

Figure S3 Characterization of TiC hollow fibre cloth supported carbon nanofibres (HFC+CNF). (a-f) SEM images. Insets are the corresponding low-magnification SEM images. (g) XRD pattern. Except for the characteristic peaks of TiC, the new broad diffraction peak centered at ~26.4 º is due to amorphous carbon (JCPDS 75-1621). (h) Raman spectrum. Two broad and low-intensity peaks (1335 and 1573 cm^{-1}) are due to amorphous carbon.

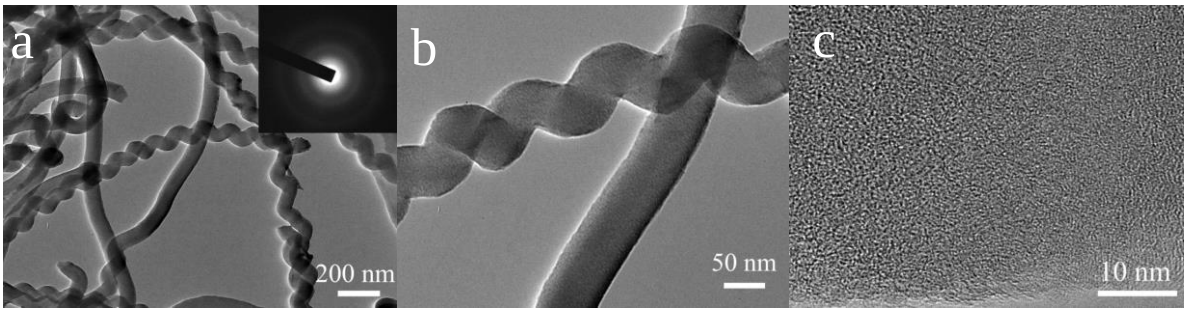

Figure S4 TEM-HRTEM images of carbon nanofibres (SAED pattern in inset). The carbon nanofibres show low-intensity selected area electronic diffraction (SAED) patterns, indicating their low crystallinity or amorphous nature. In the HRTEM image, certain incomplete fringes can be noticed revealing its low level of crystallization.

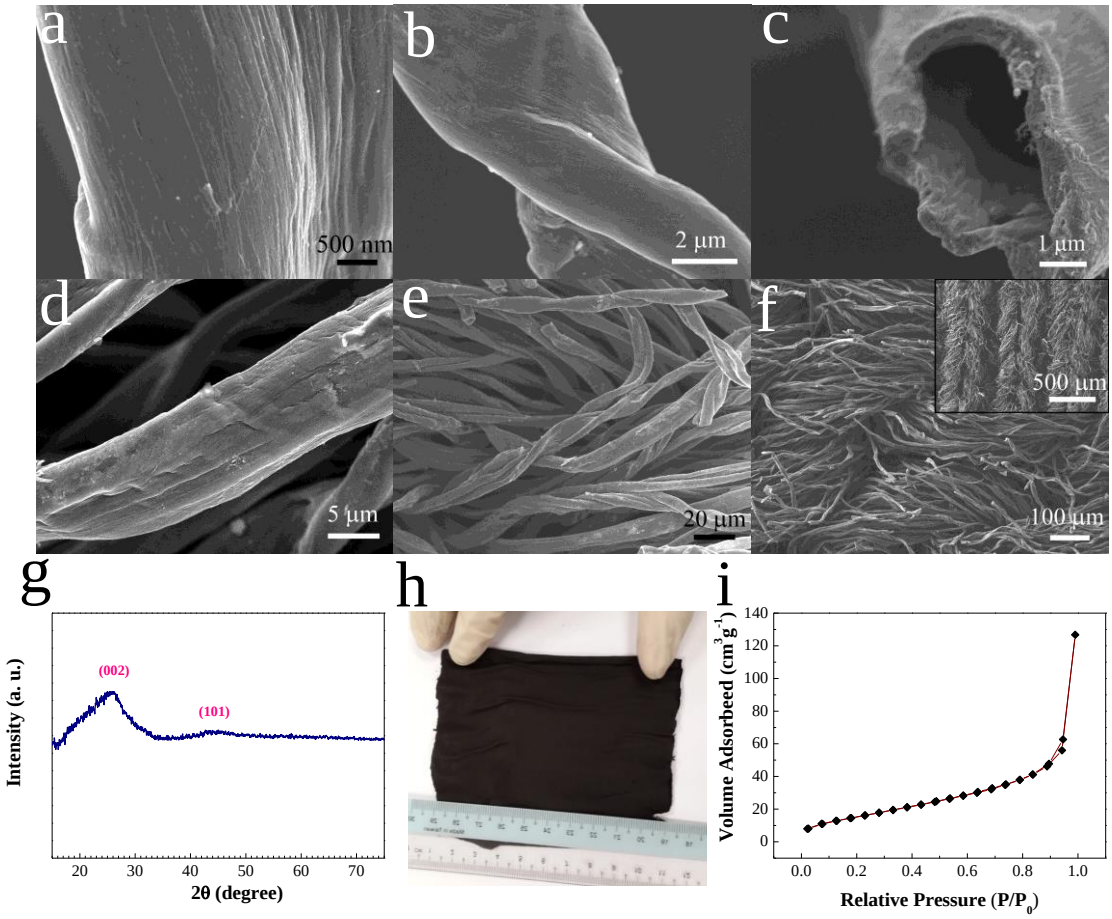

Figure S5 Characterization of carbon fibre cloth (CFC) electrodes. (a-f) SEM images. (g) XRD pattern. (h) Photograph of the electrodes. (i) BET measurement (isothermal curve). The CFC electrodes have a surface area of ~53 m^2/g.

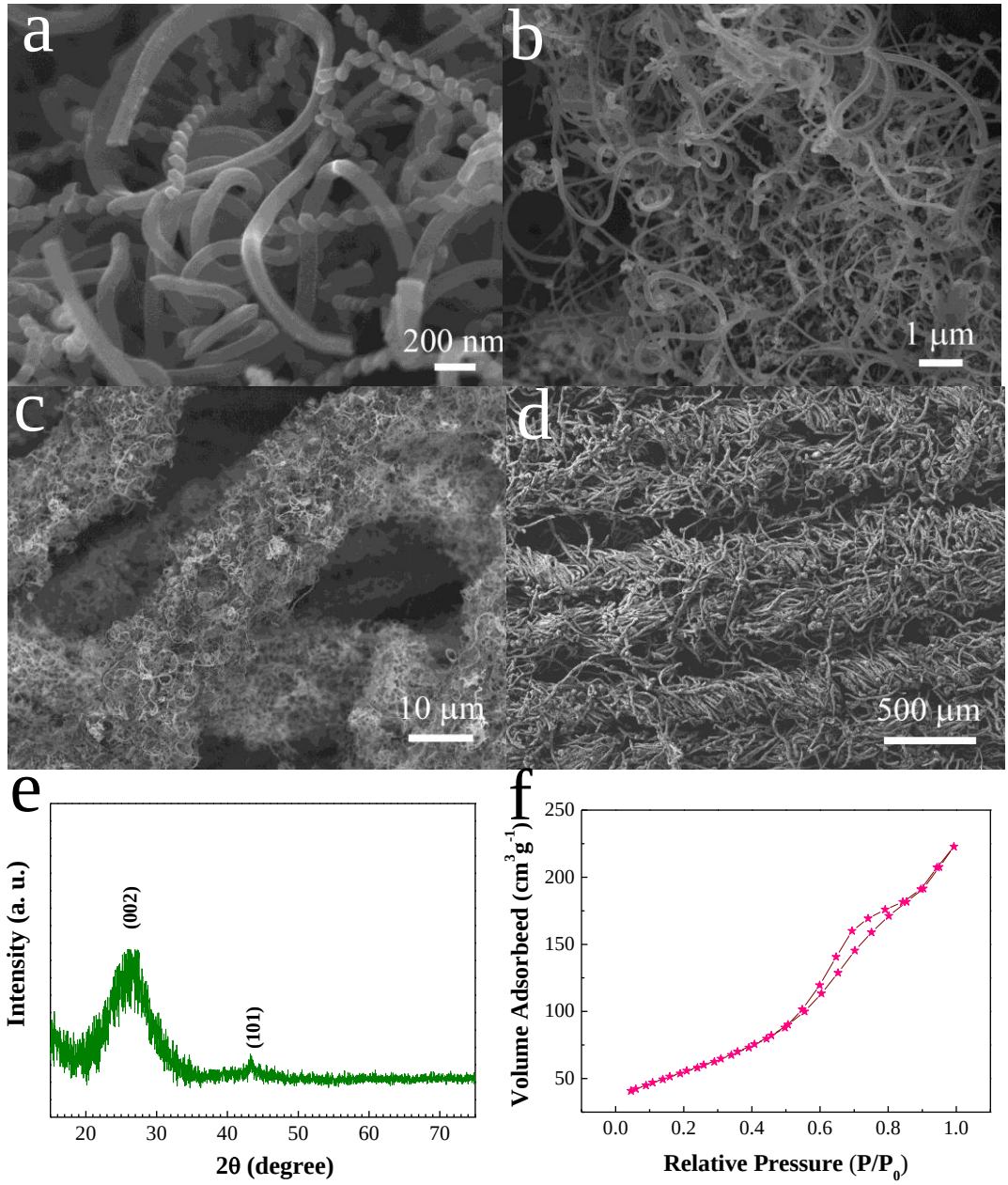

Figure S6 Characterization of carbon fibre cloth supported carbon nanofibres (CFC+CNF) electrodes. (a-d) SEM images. (e) XRD pattern. (f) BET measurement (isothermal curve). The CFC+CNF electrodes have a surface area of ~135 m^2/g.

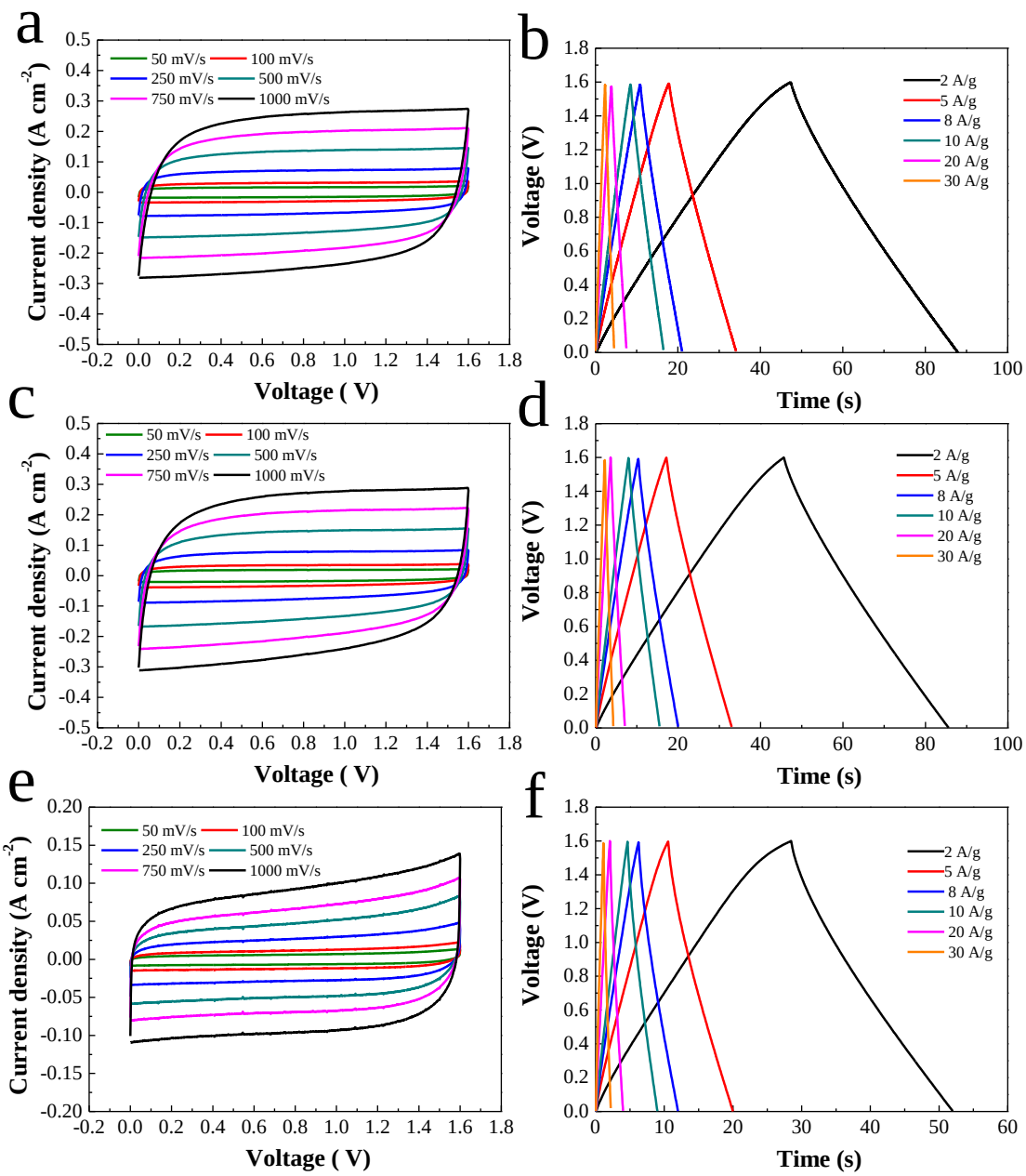

Figure S7 CV curves and charge/discharge curves of four supercapacitors based on different electrodes at room temperature (25 ºC): (a, b) TiC HFC; (c, d) CFC+CNF; (e, f) CFC.

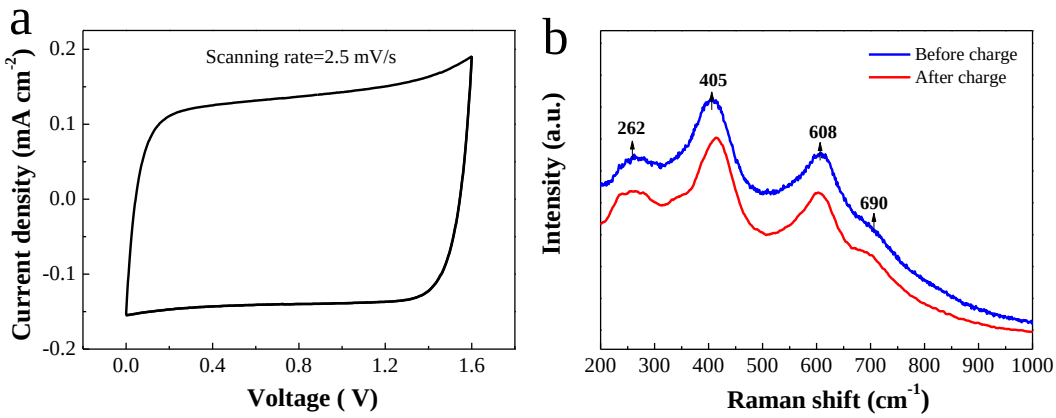

Figure S8 (a) CV curve of TiC HFNT electrode at a scanning rate of 2.5 mV/s; (b) Raman spectra of TiC electrode before and after charging at 2 A/g.

In order to further confirm whether the TiC behavors as an EDLC material, we further conducted CV test at a low scanning rate of 2.5 mV/s and Raman measurement before and after charging at 2 A/g (Fig. S8). Note that still no redox peaks can be observed in the CV curve of TiC at a low scanning rate, and the CV loop still has a quasi-rectangular shape, which is a characteristic CV behavior of EDLC materials. This is different from that of pseudo-capacitive materials, which always show obvious redox peaks in the CV at low scanning rates (especially lower than 5 mV/s). In addition, the Raman spectra of the TiC electrode before and after charging (Fig. S8b) show that no additional peaks after charging, and all peaks are still from TiC, implying that no new phase is formed after charging. These results verify that the TiC electrodes is indeed EDLC material, similar to other metal carbides such as TaC nanowire electrodes.[4]

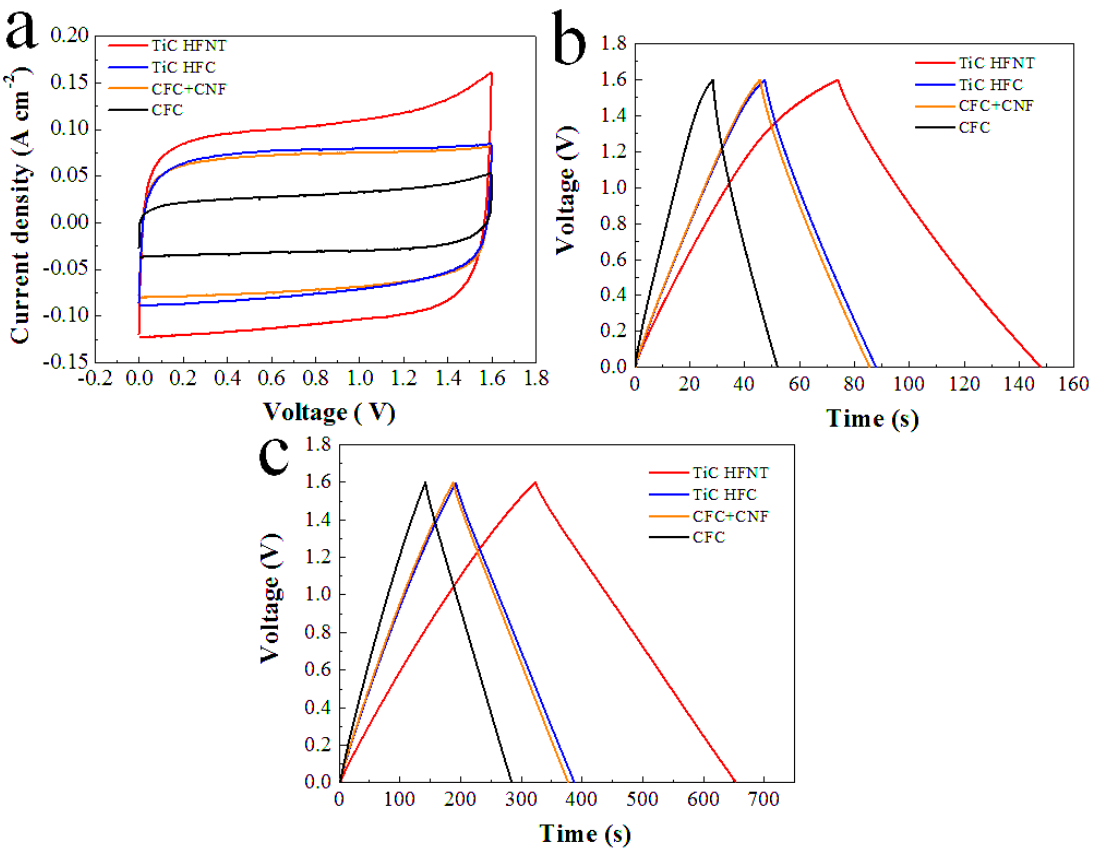

Figure S9 (a) CV curves of four supercapacitors at a scanning rate of 300 mV/s. (b) Charge/discharge curves of four supercapacitors at 2 A/g. (c) Charge/discharge curves of four supercapacitors at 0.5 A/g

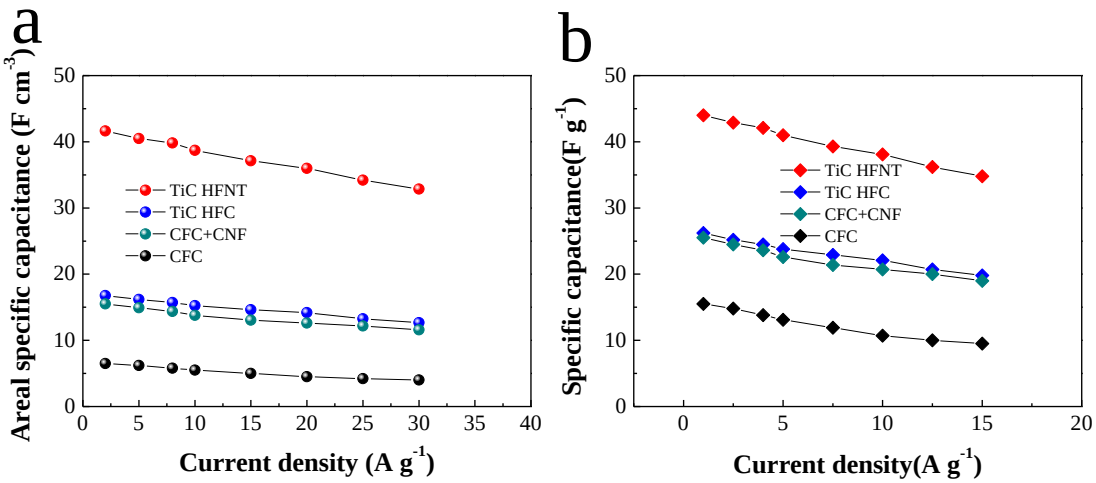

Figure S10 (a) Areal specific capacitance of four electrodes. (b) Specific capacitances of four full supercapacitors.

Table S1. Specific capacitance of four electrodes at various current densities at room temperature (25 ºC, based on the mass of single electrode).

Electrode type	Gravimetric and areal specific capacitance					
	2A/g	5A/g	8A/g	10 A/g	20 A/g	30 A/g
TiC HFNT	185 F/g	180 F/g	177 F/g	172 F/g	160 F/g	146 F/g
	41.6 F/cm^3	40.5 F/cm^3	39.8 F/cm^3	38.7 F/cm^3	36 F/cm^3	32.8 F/cm^3
TiC HFC	110 F/g	106 F/g	103 F/g	100 F/g	93 F/g	83 F/g
	16.8 F/cm^3	16.2 F/cm^3	15.7 F/cm^3	15.2 F/cm^3	14.2 F/cm^3	12.6 F/cm^3
CFC+CNF	107 F/g	103 F/g	99 F/g	95 F/g	85 F/g	74 F/g
	15.5 F/cm^3	14.9 F/cm^3	14.4 F/cm^3	13.8 F/cm^3	12.6 F/cm^3	11.6 F/cm^3
CFC	65 F/g	62 F/g	58 F/g	54 F/g	45 F/g	36 F/g
	6.5 F/cm^3	6.2 F/cm^3	5.8 F/cm^3	5.5 F/cm^3	4.5 F/cm^3	4.0 F/cm^3

Table S2 Electrochemical results of four symmetric supercapacitors at various current densities (25 ºC, based on the total mass of cathode, anode and separator).

Type	Full supercapacitors										
	Specific capacitance (F/g)						Power density (W/kg) vs. Energy density (Wh/kg)				
	1 A/g	2.5 A/g	4 A/g	5 A/g	10 A/g	15 A/g	760 W/kg	3800 W/kg	5700 W/kg	9550 W/kg	11000 W/kg
TiC HFNT	44	42.9	42.1	41	38.1	34.8	15.6	14.6	14	12.9	12.4
TiC HFC	26.2	25.2	245	23.8	22.1	19.8	9.3	8.5	8.1	7.4	7.0
CFC+ CNF	25.5	24.5	23.6	22.6	20.7	19	9	8.4	7.6	7.1	6.7
CFC	15.5	14.8	13.8	13.1	10.7	9.5	5.5	4.6	4.2	3.5	3.3

Table S3 Cycling results of four electrodes at various current densities at room temperature (25 ^{o}C, based on the mass of single electrode).

Electrode Type	**2 A/g after 50,000 cycles**	**5 A/g after 100,000 cycles**	**10 A/g after 150,000 cycles**	**2 A/g after 160,000 cycles**
TiC HFNT	183 F/g, 99 % retention	176 F/g, 98 % retention	169 F/g, 97 % retention	182 F/g,
TiC HFC	108 F/g, 98 % retention	103 F/g, 97 % retention	97 F/g, 97 % retention	107 F/g,
CFC+CNF	103 F/g, 96 % retention	94 F/g, 91 % retention	82 F/g, 86 % retention	93 F/g,
CFC	62 F/g, 95 % retention	56 F/g, 90 % retention	44 F/g, 80 % retention	54 F/g,

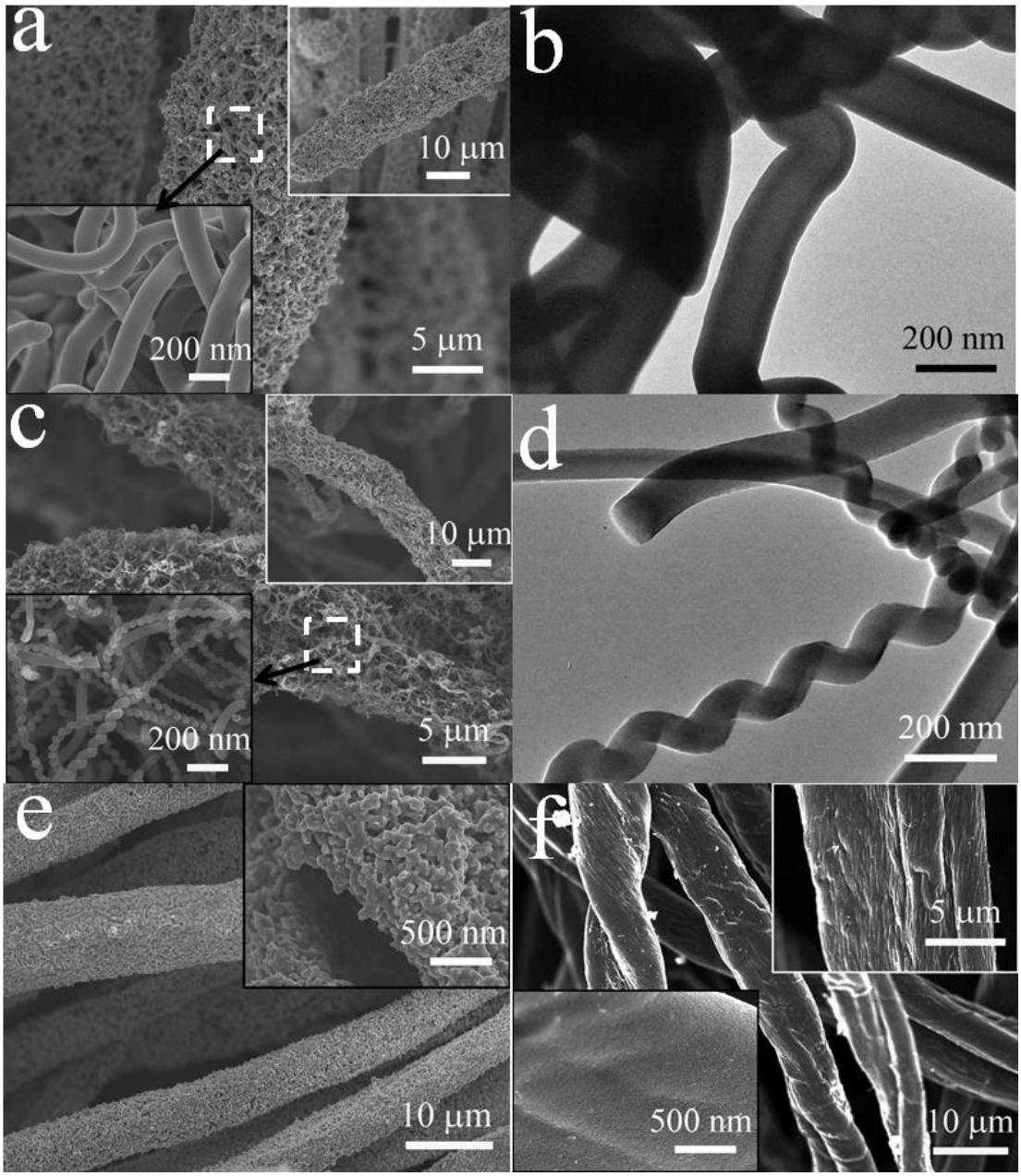

Figure S11 Morphologies of full electrodes after 160,000 cycles: (a, b) TiC HFNT electrodes; (c, d) CFC+CNF electrodes; (e) TiC HFC electrodes and (f) CFC electrodes.

Table S4 Electrochemical parameters of different kinds of carbon materials electrodes.

Carbon electrodes	Material type	Specific capacitance (F/g)	Capacitance retention after cycles	Mass density (mg cm^{-2})
Activated Carbon (AC)[5]	Powder	120-205	81% after 23,000 cycles	3
AC[6]	Powder	135	76% after 10,000 cycles	8-10
N-doped AC[7]	Powder	150	/	4
AC[8]	Powder	74	88% after 500 cycles	3-4
Single-wall carbon nanotube (SWCNT)[9]	Powder	110-180	/	11.25
SWCNT arrays [10]	Integrated electrode	80	/	0.5
SWCNT[11]	Integrated electrode	36-110	/	0.3
Carbon nanotubes (CNTs)[12]	Integrated electrode	21	/	/
AC/Graphene[13]	Powder	103-210	94.7 % after 5,000 cycles	0.3
RGO/carbon black[14]	Integrated electrode	80-112	100% after 2,000 cycles	1-2
Nano carbon[15]	Powder	180	85 % After 10,000 cycles	0.91
RGO[16-18]	Powder	97-154	/	3.7 -5
RGO paper[19]	Film	181	/	0.5
Activated graphene[20]	Powder	166	97% after 10,000 cycles	/
Carbon nano-onions [21]	Powder	76-115	89 % after 4000 cycles	/
Graphene hydrogel[22]	Integrated electrode	110-119	/	/
Graphene [23]	Integrated electrode	100-139	61 % after 700 cycles	0.6-0.8
Graphene[24]	Integrated electrode	60-70	100% after 1000 cycles	0.2

Graphene [25]	Integrated electrode	265	98 % after 10,000 cycles	0.6
Graphene[26-28]	Powder	159-180	98 % after 1000 cycles	2.1
Graphene[29, 30]	Powder	110-256	99 % after 5000 cycles	2
Sponge-like Graphene[31]	Powder	50-65	/	2
Graphene paper[32]	Integrated electrode	160-212	84 % after 2000 cycles	8
Graphene aerogel[33]	Integrated electrode	186-366	80 % after 2000 cycles	1
Carbon nanofiber[34]	Integrated electrode	130-180	90% after 3000 cycles	60
Mesoporous carbon fiber[35]	Powder	200-300	98% after 1000 cycles	0.125
Carbon spheres/graphene composites[36]	Powder	198	95% after 1000 cycles	4.1
Laser-scribed Graphene[37]	Integrated electrode	100-300	>97 % after 10,000 cycles	0.036
CNTs/Graphene composites[38]	Powder	385	100 % after 2,000 cycles	0.9
Graphene/ CNTs composites[39]	Powder	326.5	/	0.8
3D graphene[40]	Powder	166-341	96 % after 1,000 cycles	0.3-0.4
CNTs/RGO composites[41]	Powder	244	100 % after 1,000 cycles	2
Nitrogen-doped graphene hollow nanospheres[42]	Powder	381	96 % after 5,000 cycles	0.11
Carbon nanocage[43]	Powder	185	91.7 % after 10,000 cycles	0.2
Mesoporous carbon fibres[44]	Powder	280	91.6 % after 1,000 cycles	1-2
Nitrogen-doped porous carbon nanofibres[45]	Powder	202	100 % after 3,000 cycles	5-6

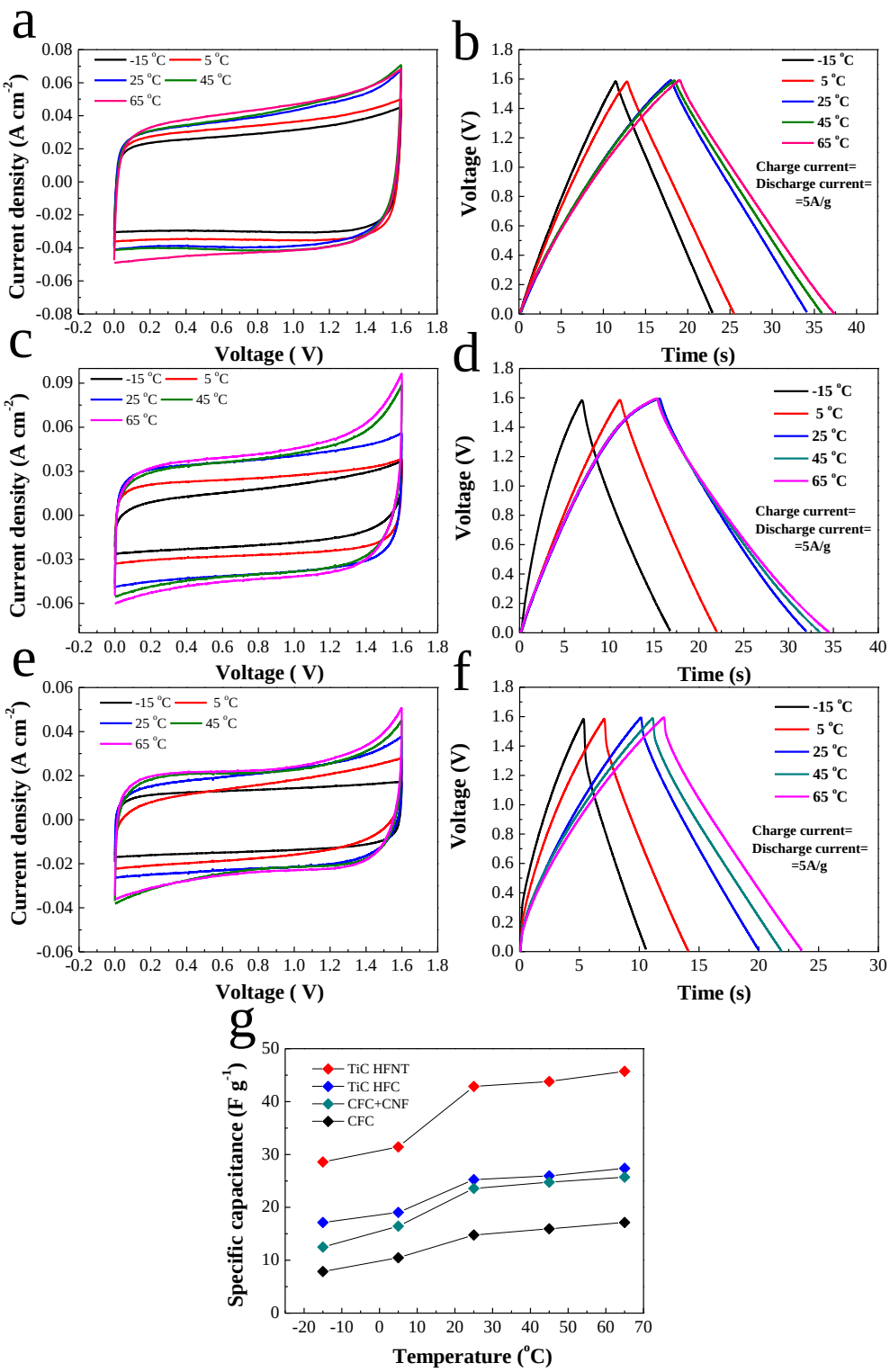

Figure S12 CV curves (a scanning rate of 200 mV/s) and charge/discharge curves of four supercapacitors (a current density of 5A/g) at different working temperatures ranging from −15 °C to 65 °C: (a, b) TiC HFC; (c, d) CFC+CNF; (e, f) CFC. (g) Specific capacitances of full supercapacitors at different working temperatures.

Table S5 Electrochemical results of four electrodes and symmetric supercapacitors at current density of 5 A/g at different working temperatures.

Electrode type	–15 ºC	5 ºC	25 ºC	45 ºC	65 ºC
TiC HFNT	Single electrode				
	120 F/g	132 F/g	180 F/g	184 F/g	192 F/g
	Full supercapacitor				
	28.6 F/g	31.4 F/g	42.8 F/g	43.8 F/g	45.7 F/g
TiC HFC	Single electrode				
	72 F/g	80 F/g	106 F/g	109 F/g	115 F/g
	Full supercapacitor				
	17.1 F/g	19.0 F/g	25.2 F/g	26 F/g	27.4
CFC+ CNF	Single electrode				
	53 F/g	69 F/g	99 F/g	104 F/g	108 F/g
	Full supercapacitor				
	12.5 F/g	16.4 F/g	23.6 F/g	24.7 F/g	25.7 F/g
CFC	Single electrode				
	33 F/g	44 F/g	62 F/g	67 F/g	72 F/g
	Full supercapacitor				
	7.9 F/g	10.5 F/g	14.8 F/g	16 F/g	17.1 F/g

Table S6 Cycling results of four electrodes at 5 A/g at −15 °C and 65 °C (based on the mass of single electrode).

Electrode type	5 A/g after 50,000 cycles at −15 °C		5 A/g after 100,000 cycles at 65 °C
TiC HFNT	115 F/g, 95. 8 % retention		178 F/g, 93.5 % retention
TiC HFC	70 F/g, 97.2 % retention		105 F/g, 91.3 % retention
CFC+CNF	45 F/g, 84.9 % retention		80 F/g, 74.1 % retention
CFC	25 F/g, 75.7 % retention		41 F/g, 56.9 % retention

References

1. V. Kiran, K. L. Nagashree and S. Sampath, *RSC Adv.* , 2014, 4, 12057-12064.
2. B. H. Lohse, A. Calka and D. Wexler, *J. Appl. Phys.*, 2005, 97.
3. L. H. Zhang and R. V. Koka, *Mater. Chem. Phys.*, 1998, 57, 23-32.
4. X. Y. Tao, J. Du, Y. P. Li, Y. C. Yang, Z. Fan, Y. P. Gan, H. Huang, W. K. Zhang, L. X. Dong and X. D. Li, *Adv. Energy Mater.*, 2011, 1, 534-539.
5. V. Ruiz, C. Blanco, R. Santamaría, J. Ramos-Fernández, M. Martínez-Escandell, A. Sepúlveda-Escribano and F. Rodríguez-Reinoso, *Carbon*, 2009, 47, 195-200.
6. L. Demarconnay, E. Raymundo-Pinero and F. Béguin, *Electrochem. Commun.*, 2010, 12, 1275-1278.
7. D. Hulicova-Jurcakova, M. Seredych, G. Q. Lu and T. J. Bandosz, *Adv. Funct. Mater.*, 2009, 19, 438-447.
8. V. Subramanian, C. Luo, A. Stephan, K. Nahm, S. Thomas and B. Wei, *J. Phys. Chem. C*, 2007, 111, 7527-7531.
9. K. H. An, W. S. Kim, Y. S. Park, J.-M. Moon, D. J. Bae, S. C. Lim, Y. S. Lee and Y. H. Lee, *Adv. Funct. Mater.*, 2001, 11, 387-392.
10. D. N. Futaba, K. Hata, T. Yamada, T. Hiraoka, Y. Hayamizu, Y. Kakudate, O. Tanaike, H. Hatori, M. Yumura and S. Iijima, *Nat. Mater.*, 2006, 5, 987-994.
11. M. Kaempgen, C. K. Chan, J. Ma, Y. Cui and G. Gruner, *Nano Lett.*, 2009, 9, 1872-1876.
12. C. Du and N. Pan, *Nanotechnology*, 2006, 17, 5314.
13. C. Zheng, X. Zhou, H. Cao, G. Wang and Z. Liu, *J. Power Sources*, 2014, 258, 290-296.

14. Y. Wang, J. Chen, J. Cao, Y. Liu, Y. Zhou, J.-H. Ouyang and D. Jia, *J. Power Sources*, 2014, 271, 269-277.
15. E. Raymundo-Piñero, F. Leroux and F. Béguin, *Adv. Mater.* , 2006, 18, 1877-1882.
16. M. D. Stoller, S. Park, Y. Zhu, J. An and R. S. Ruoff, *Nano Lett.*, 2008, 8, 3498-3502.
17. S. R. C. Vivekchand, C. S. Rout, K. S. Subrahmanyam, A. Govindaraj and C. N. R. Rao, *Journal of Chemical Sciences*, 2008, 120, 9-13.
18. C. Liu, Z. Yu, D. Neff, A. Zhamu and B. Z. Jang, *Nano Lett.*, 2010, 10, 4863-4868.
19. Z. Bo, W. Zhu, X. Tu, Y. Yang, S. Mao, Y. He, J. Chen, J. Yan and K. Cen, *J. Phys. Chem. C*, 2014, 118, 13493-13502.
20. Y. Zhu, S. Murali, M. D. Stoller, K. Ganesh, W. Cai, P. J. Ferreira, A. Pirkle, R. M. Wallace, K. A. Cychosz and M. Thommes, *Science*, 2011, 332, 1537-1541.
21. Y. Gao, Y. S. Zhou, M. Qian, X. N. He, J. Redepenning, P. Goodman, H. M. Li, L. Jiang and Y. F. Lu, *Carbon*, 2013, 51, 52-58.
22. P. Chen, J.-J. Yang, S.-S. Li, Z. Wang, T.-Y. Xiao, Y.-H. Qian and S.-H. Yu, *Nano Energy*, 2013, 2, 249-256.
23. Y. Chen, X. Zhang, P. Yu and Y. Ma, *J. Power Sources*, 2010, 195, 3031-3035.
24. W. Chen, Z. Fan, G. Zeng and Z. Lai, *J. Power Sources*, 2013, 225, 251-256.
25. Z. Huang, H. Zhang, Y. Chen, W. Wang, Y. Chen and Y. Zhong, *Electrochim. Acta*, 2013, 108, 421-428.
26. Z. Xiong, C. Liao and X. Wang, *J. Mater. Chem.A*, 2014, 2, 19141-19144.
27. P. Wen, P. Gong, Y. Mi, J. Wang and S. Yang, *RSC Adv.* , 2014, 4, 35914-35918.
28. J. W. Lee, J. M. Ko and J.-D. Kim, *Electrochim. Acta*, 2012, 85, 459-466.
29. H. Wang, Y. Wang, Z. Hu and X. Wang, *ACS Appl. Mat. Interfaces*, 2012, 4, 6827-6834.
30. L. G. Bulusheva, V. A. Tur, E. O. Fedorovskaya, I. P. Asanov, D. Pontiroli, M. Riccò and A. V. Okotrub, *Carbon*, 2014, 78, 137-146.
31. Z. Xu, Z. Li, C. M. B. Holt, X. Tan, H. Wang, B. S. Amirkhiz, T. Stephenson and D. Mitlin, *J. Phys. Chem. Lett.*, 2012, 3, 2928-2933.
32. D. Sun, X. Yan, J. Lang and Q. Xue, *J. Power Sources*, 2013, 222, 52-58.
33. S. Ye, J. Feng and P. Wu, *ACS Appl. Mat. Interfaces*, 2013, 5, 7122-7129.
34. J. R. McDonough, J. W. Choi, Y. Yang, F. La Mantia, Y. Zhang and Y. Cui, *Appl. Phys. Lett.*, 2009, 95, 243109.
35. Y. Liang, X. Feng, L. Zhi, U. Kolb and K. Müllen, *Chem. Commun.* , 2009, 809-811.
36. C. Xian áGuo and C. Ming âLi, *Energy Environ. Sci.*, 2011, 4, 4504-4507.
37. M. F. El-Kady, V. Strong, S. Dubin and R. B. Kaner, *Science*, 2012, 335, 1326-1330.
38. Z. Fan, J. Yan, L. Zhi, Q. Zhang, T. Wei, J. Feng, M. Zhang, W. Qian and F. Wei, *Adv. Mater.* , 2010, 22, 3723-3728.
39. S.-Y. Yang, K.-H. Chang, H.-W. Tien, Y.-F. Lee, S.-M. Li, Y.-S. Wang, J.-Y. Wang, C.-C. M. Ma and C.-C. Hu, *J. Mater. Chem.*, 2011, 21, 2374-2380.

40. J. Hu, Z. Kang, F. Li and X. Huang, *Carbon*, 2014, 67, 221-229.
41. F. Zeng, Y. Kuang, N. Zhang, Z. Huang, Y. Pan, Z. Hou, H. Zhou, C. Yan and O. G. Schmidt, *J. Power Sources*, 2014, 247, 396-401.
42. W. Fan, Y.-Y. Xia, W. W. Tjiu, P. K. Pallathadka, C. He and T. Liu, *J. Power Sources*, 2013, 243, 973-981.
43. K. Xie, X. T. Qin, X. Z. Wang, Y. N. Wang, H. S. Tao, Q. Wu, L. J. Yang and Z. Hu, *Adv. Mater.* , 2012, 24, 347-352.
44. W. Li, F. Zhang, Y. Q. Dou, Z. X. Wu, H. J. Liu, X. F. Qian, D. Gu, Y. Y. Xia, B. Tu and D. Y. Zhao, *Adv. Energy Mater.*, 2011, 1, 382-386.
45. L. F. Chen, X. D. Zhang, H. W. Liang, M. G. Kong, Q. F. Guan, P. Chen, Z. Y. Wu and S. H. Yu, *ACS Nano*, 2012, 6, 7092-7102.